nature climate change

SUPPLEMENTARY INFORMATION
https://doi.org/10.1038/s41558-017-0066-9

In the format provided by the authors and unedited.

Greenhouse gas emissions from diverse Arctic Alaskan lakes are dominated by young carbon

Clayton D. Elder[1*], Xiaomei Xu[1], Jennifer Walker[1], Jordan L. Schnell[1,7], Kenneth M. Hinkel[2,8], Amy Townsend-Small[3], Christopher D. Arp[4], John W. Pohlman[5], Benjamin V. Gaglioti[6] and Claudia I. Czimczik[1*]

[1]Department of Earth System Science, University of California, Irvine, CA, USA. [2]Department of Geography, University of Cincinnati, Cincinnati, OH, USA. [3]Department of Geology, University of Cincinnati, Cincinnati, OH, USA. [4]Water and Environmental Research Center, University of Alaska, Fairbanks, AK, USA. [5]USGS Woods Hole Coastal and Marine Science Center, Woods Hole, MA, USA. [6]Lamont–Doherty Earth Observatory of Columbia University, Palisades, NY, USA. Present addresses: [7]Department of Earth and Planetary Sciences, Northwestern University, Evanston, IL, USA. [8]Geological and Mining Engineering and Sciences, Michigan Technological University, Houghton, MI, USA. *e-mail: cdelder@uci.edu; czimczik@uci.edu

Greenhouse gas emissions from diverse Arctic Alaskan lakes are dominated by young carbon

Authors:

Clayton D. Elder[1]*, Xiaomei Xu[1], Jennifer Walker[1], Jordan L. Schnell[1]†, Kenneth M. Hinkel[2]‡, Amy Townsend-Small[3], Christopher D. Arp[4], John W. Pohlman[5], Benjamin V. Gaglioti[6], Claudia I. Czimczik[1]*

Supplementary Information:

Supplementary Figures:

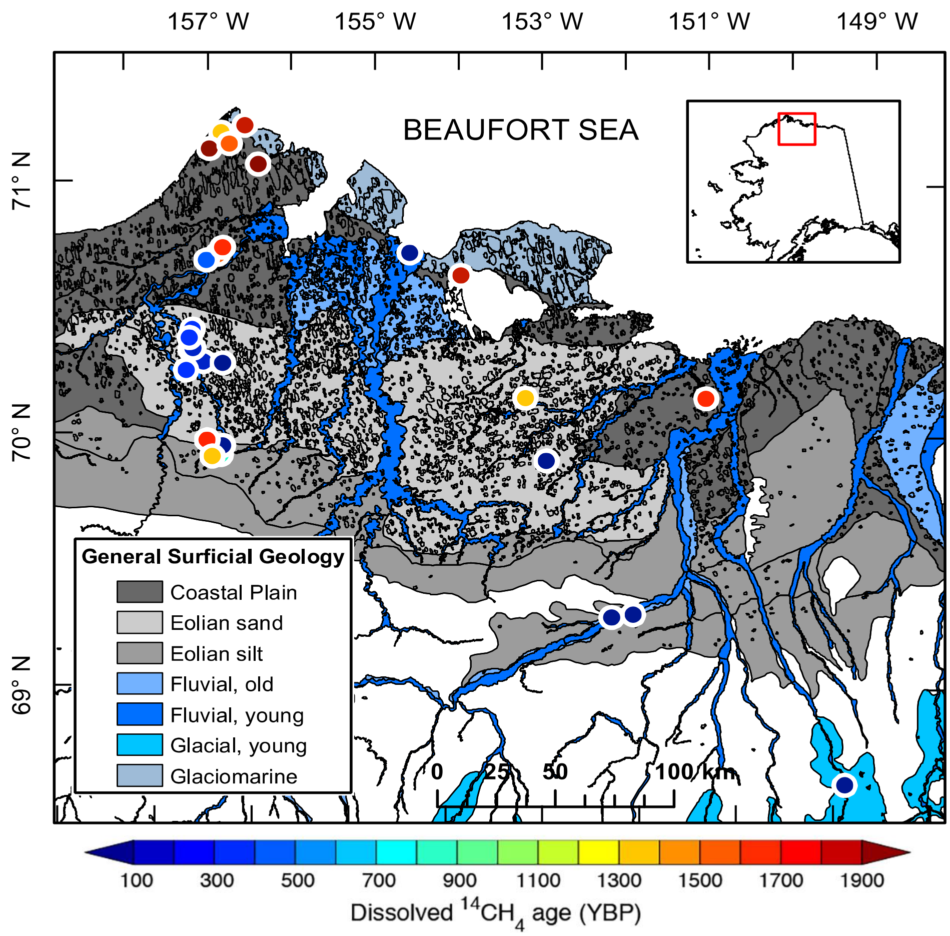

Figure S1: North Slope general surficial geology with dissolved $^{14}CH_4$ age observations and lake distribution. This map depicts the mean observed ^{14}C age of dissolved CH_4 in 27 lakes (as in Figure 3) (n = 1-2 measurements per lake), general surficial geology boundaries as determined by Jorgenson et al. 2014[35], and lakes greater than 0.5 km^2. White areas represent un-observed geologic units or the Beaufort Sea.

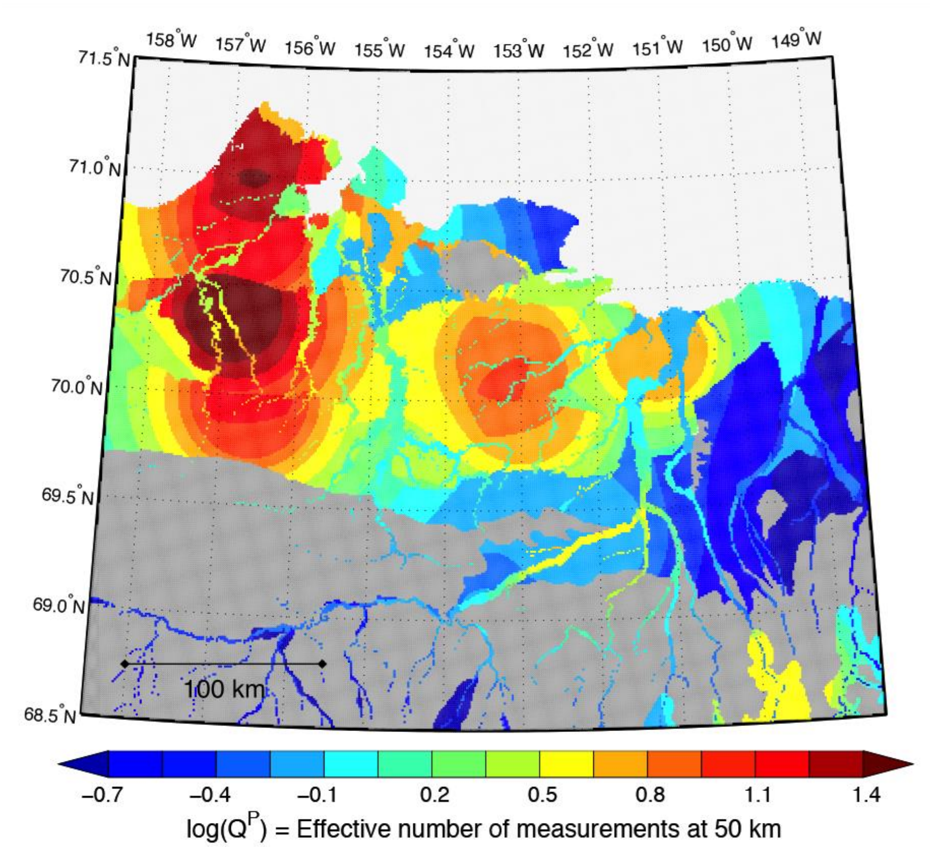

Figure S2: Uncertainty of spatial interpolation of the ^{14}C ages of lake-dissolved CH_4. The map shows the logarithm of the quality of prediction (Q^P) of mean $^{14}CH_4$ ages in lakes, interpolated by inverse distance weighing with a weight reduction parameter for predictions in non-similar geology categories. Q^P is defined as the effective number of measurements at a distance of 50 km (Equation 12). Smaller values indicate greater uncertainty of prediction. Note that values can exceed the total number of sites (n = 27) when measured-to-predicted distances are less than 50 km (see Methods).

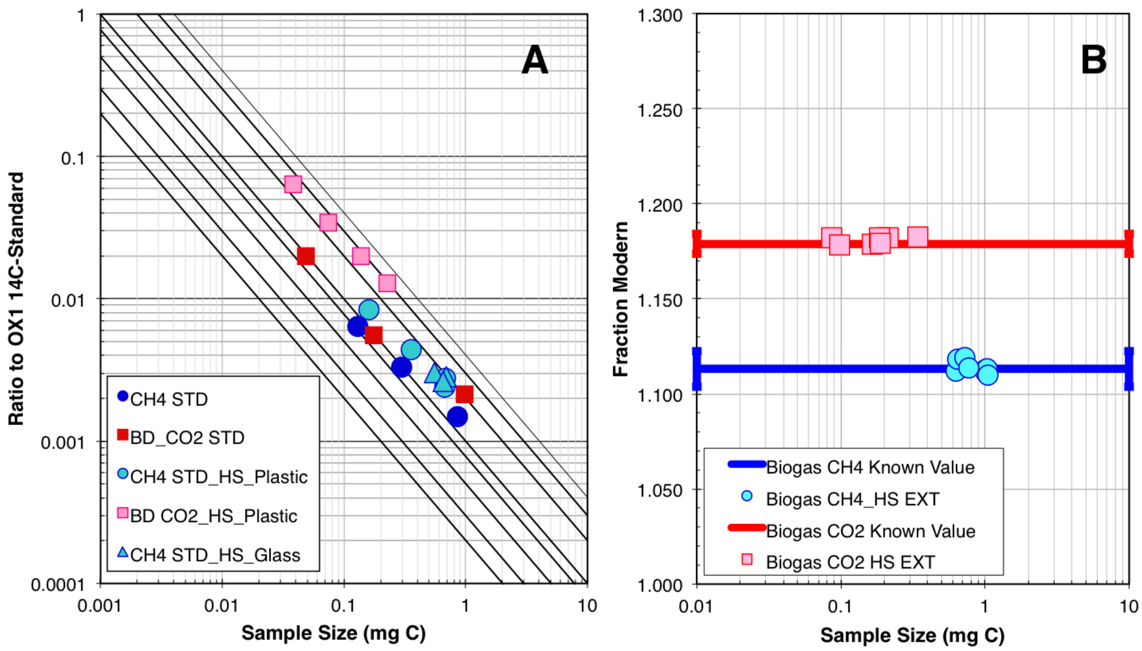

Figure S3: ^{14}C isotopic blank and precision assessment of the winter sample collection method for dissolved $^{14}CH_4$ and $^{14}CO_2$. A) The $^{14}C/^{12}C$ ratio to the OX1 ^{14}C standard in different sizes of ^{14}C-free CH_4 (circles) and CO_2 (squares) standards analyzed with the headspace extraction method (HS) and by direct combustion (STD). Pure gases directly combusted (STD) are shown as darker color symbols and headspace extractions as lighter colors (HS). From left to right, the solid diagonal lines represent the mass-balance effect of 0.2, 0.3, 0.5, 0.8, 1.0, 2.0, 3.0 and 4.0 µg of modern extraneous C in the total sample size. The modern C blanks introduced by this method are approximately 1.5 µg C and 2.5 µg C for CH_4 and CO_2, respectively. B) The fraction modern of different sized biogas CH_4 and CO_2 ^{14}C lab standards. Variation in biogas samples, prepared by headspace extraction method: FM CH_4 = 1.1138 ± 0.0032 (± std. dev., n=8); and FM CO_2 = 1.1807 ± 0.0019 (± std. dev., n=7). Solid horizontal lines and error bars represent mean and range of biogas standards measured via direct combustion (n = 20).

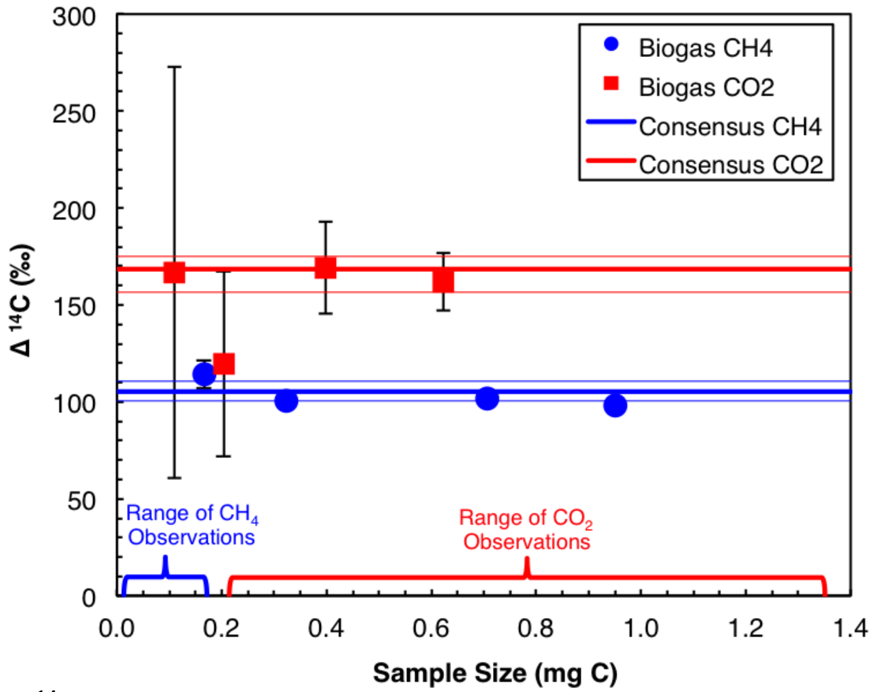

Figure S4: ^{14}C isotopic blank and precision assessment of the summer sample collection method (Liqui-Cel) for dissolved $^{14}CH_4$ and $^{14}CO_2$. Results depict the mass-corrected biogas lab standards following a one-hour recirculation and extraction through the Liqui-Cel gas extraction system. Error bars represent the effect of mass correction with 2 ± 1 μg extraneous ^{14}C-free C for CH_4 and 25 ± 7.5 μg ^{14}C-free C for CO_2. This mass correction and associated error was applied to all North Slope dissolved CH_4 and CO_2 values produced in August 2014 from the Liqui-Cel extraction system. The North Slope sample yield ranges for dissolved CH_4 and CO_2 in August 2014 are shown in the plot with the blue and red brackets, respectively. Thick and thin horizontal lines depict the mean and range of 20 biogas CH_4 and CO_2 measurements via direct combustion and analysis, respectively.

Supplementary Tables:

Table S1: Location, physical and chemical properties of 40 lakes on the North Slope of Alaska, USA. With Lat – latitude, long – longitude, Depth – mean depth, Area – surface area, Lake Origin – lake forming process, Geology – underlying substrate, pH (August 2014) – summer pH, T (August 2014) – summer temperature. Lakes identified as "quasi-thermokarst" indicate water bodies where basin initiation is uncertain and may have occurred via non-thermokarst processes, but currently interact with the surrounding permafrost terrain[61]. The minimum number of annual samples collected between 2012 and 2014 is shown by (n). TK = thermokarst. n.m. = not measured.

Lake ID	n	Lat. N	Long. W	Depth	Area	Lake Origin	Geology	pH (August)	Temp. (August)
		D.D.	*D.D.*	*m*	*ha*				*°C*
BRW 100	2	71.24163	-156.77391	1.83	183.82	TK	Coastal Plain	6.09	6.90
BRW 103	2	71.12312	-156.31664	1.46	179.81	TK	Coastal Plain	n.m.	n.m.
BRW 104	1	71.19358	-156.50224	1.05	174.53	TK	Coastal Plain	n.m.	n.m.
BRW 106	2	71.17556	-156.89731	1.36	363.16	TK	Coastal Plain	n.m.	n.m.
BRW 107	2	71.27396	-156.49700	1.61	124.98	TK	Glaciomarine	7.30	6.83
BRW 130	2	71.19909	-156.66536	1.19	296.84	TK	Coastal Plain	7.68	6.60
LMR 402	2	70.72825	-156.84290	1.00	356.00	TK	Coastal Plain	7.11	10.40
LMR 403	1	70.78256	-156.66823	1.07	168.11	TK	Coastal Plain	n.m.	n.m.
LMR 400	1	70.75409	-156.72044	1.03	252.30	TK	Coastal Plain	n.m.	n.m.
ATQ 200	2	70.45475	-156.94790	1.07	271.30	Quasi-TK	Eolian Sand	6.44	10.30
ATQ 201	2	70.32723	-156.80655	1.07	145.53	Quasi-TK	Eolian Sand	n.m.	n.m.
ATQ 202	2	70.28790	-156.98490	1.20	148.81	Quasi-TK	Eolian Sand	n.m.	n.m.
ATQ 204	2	70.37249	-156.96270	0.88	40.34	Quasi-TK	Eolian Sand	n.m.	n.m.
ATQ 205	2	70.37770	-156.92665	0.99	150.89	Quasi-TK	Eolian Sand	n.m.	n.m.
ATQ 206	2	70.41557	-156.98128	1.23	183.05	Quasi-TK	Eolian Sand	n.m.	n.m.
ATQ 207	2	70.32911	-156.59154	0.80	353.61	Quasi-TK	Eolian Sand	n.m.	n.m.
RDC 300	2	69.96079	-156.54585	2.31	63.82	TK	Eolian Silt	n.m.	n.m.
RDC 306	2	69.99649	-156.52992	1.55	44.73	TK	Fluvial, young	n.m.	n.m.
RDC 308	2	69.98635	-156.42445	2.59	78.74	TK	Eolian Silt	8.04	10.30
RDC 309	2	70.02459	-156.56652	1.78	57.26	TK	Eolian Sand	n.m.	n.m.
RDC 311	2	69.99614	-156.68912	3.13	76.93	TK	Eolian Silt	n.m.	n.m.
RDC 310	1	70.01736	-156.69791	1.51	202.81	TK	Eolian Silt	7.15	10.80
RDC 312	2	69.95348	-156.63817	2.32	75.17	TK	Eolian Silt	n.m.	n.m.
TOO 005	1	68.64916	-149.84899	1.20	0.56	Kettle	Glacial Young	n.m.	n.m.

TOO 006	1	68.65247	-149.59947	5.24	2.18	Kettle	Glacial Young	n.m.	n.m.
INI 001	1	69.99615	-153.07007	5.61	66.41	Quasi-TK	Eolian Sand	n.m.	n.m.
INI 004	1	70.01033	-153.15491	3.94	172.46	Quasi-TK	Fluvial Young	n.m.	n.m.
INI 005	1	70.01843	-153.18606	1.47	4.89	Oxbow	Fluvial Young	n.m.	n.m.
L9811	1	70.20547	-151.17980	1.90	417.61	TK	Coastal Plain	n.m.	n.m.
INI 003	1	69.95922	-152.95072	1.44	417.27	Quasi-TK	Eolian Sand	n.m.	n.m.
INI 006	1	70.21893	-153.17164	4.23	361.75	Quasi-TK	Eolian Sand	n.m.	n.m.
IKP 003	1	70.79303	-154.51704	2.86	11.22	TK	Fluvial Young	n.m.	n.m.
IKP 001	1	70.78966	-154.45043	2.61	68.68	TK	Fluvial Young	n.m.	n.m.
TES 001	1	70.76625	-153.56248	2.23	979.90	TK	Glaciomarine	n.m.	n.m.
TES 004	1	70.69273	-153.73894	6.20	83613.66	TK	Freshwater	n.m.	n.m.
TES 006	1	70.70613	-153.92424	2.19	110.15	TK	Coastal Plain	n.m.	n.m.
UMI 001	1	69.28254	-152.16701	1.83	59.45	TK	Eolian Silt	n.m.	n.m.
UMI 003	1	69.35533	-152.01769	1.74	11.60	Quasi-TK	Fluvial Old	n.m.	n.m.
UMI 005	1	69.34589	-152.24869	2.10	1.61	Oxbow	Fluvial Young	n.m.	n.m.
UMI 006	1	69.27923	-152.12693	2.12	9.22	TK	Eolian Silt	n.m.	n.m.

Table S2: Concentration and isotopic composition of dissolved CH_4 and CO_2 in 40 lakes on the North Slope of Alaska. Data is shown as average ± standard deviation (SD) when n = 2 (sampled in 2013 and 2014), or if n = 1, the measurement error is shown. Winter = W, Summer = S. n.m. = not measured.

Name	**[CH_4]**	**±**	**[CH_4]**	**±**	**^{14}C-CH_4**	**±**	**^{14}C-CH_4**	**±**	**$\delta^{13}C$-CH_4**	**±**	**[CO_2]**	**±**	**[CO_2]**	**±**	**^{14}C-CO_2**	**±**	**^{14}C-CO_2**	**±**	**$\delta^{13}C$-CO_2**	**±**
	W	**n=2, SD**	**S**		**W**	**n=2, SD**	**S**		**W**	**n=2, SD**	**W**	**n=2, SD**	**S**		**W**	**n=2, SD**	**S**		**W**	**n=2, SD**
	µmol/ L	***n=1, error***	***µmol/ L***	***n=1, error***	***FM***	***n=1, error***	***FM***	***n=1, error***	***‰***	***n=1, error***	***µmol/ L***	***n=1, error***	***µmol/ L***	***n=1, error***	***FM***	***n=1, error***	***FM***	***n=1, error***	***‰***	***n=1, error***
BRW 100	6.64	0.51	0.59	0.01	0.848	0.016	0.894	0.025	n.m.	n.m.	156.8	11.5	113.5	2.3	0.908	0.006	1.096	0.045	-24.3	2.5
BRW 103	78.46	110.40	n.m.	n.m.	0.766	0.001	n.m.	n.m.	-70.9	0.1	911.3	826.9	n.m.	n.m.	0.839	0.002	n.m.	n.m.	-20.5	0.3
BRW 104	0.20	0.01	n.m.	n.m.	n.m.	n.m.	n.m.	n.m.	n.m.	n.m.	545.5	5.5	n.m.	n.m.	0.901	0.002	n.m.	n.m.	n.m.	n.m.
BRW 106	29.93	25.98	n.m.	n.m.	0.780	0.002	n.m.	n.m.	-44.0	35.3	769.9	387.6	n.m.	n.m.	0.866	0.005	n.m.	n.m.	-21.0	0.1
BRW 107	38.32	47.65	0.51	0.01	0.797	0.016	0.805	0.005	-63.2	0.1	720.2	301.8	12.2	0.2	0.831	0.015	0.974	0.013	-23.3	2.8
BRW 130	79.15	76.34	0.24	0.02	0.822	0.008	0.843	0.015	-52.6	23.8	700.6	275.9	30.1	0.6	0.895	0.007	0.988	0.010	-17.8	0.1
LMR 400	28.25	5.93	n.m.	n.m.	0.826	0.005	n.m.	n.m.	-65.8	0.6	1404.5	242.3	n.m.	n.m.	0.902	0.006	n.m.	n.m.	-11.6	0.5
LMR 402	352.16	3.52	0.27	0.02	0.939	0.001	0.961	0.014	-63.4	0.1	927.6	9.3	42.7	0.9	0.962	0.001	n.m.	n.m.	-13.3	0.5
LMR 403	65.28	0.65	n.m.	n.m.	0.812	0.002	n.m.	n.m.	-65.8	0.1	523.7	5.2	n.m.	n.m.	0.884	0.002	n.m.	n.m.	-16.1	0.5
ATQ 200	27.98	33.40	0.18	0.01	0.979	0.053	1.031	0.014	-39.5	0.1	273.4	284.7	70.4	1.4	1.015	0.000	1.046	0.009	-17.5	0.5
ATQ 201	67.59	95.21	n.m.	n.m.	0.980	0.003	n.m.	n.m.	-60.7	0.1	353.2	31.8	n.m.	n.m.	0.990	0.002	n.m.	n.m.	-13.9	3.1
ATQ 202	29.93	41.30	n.m.	n.m.	0.973	0.003	n.m.	n.m.	-38.8	0.1	218.8	164.7	n.m.	n.m.	0.994	0.006	n.m.	n.m.	-11.9	0.5
ATQ 204	352.95	481.86	n.m.	n.m.	0.992	0.015	n.m.	n.m.	n.m.	n.m.	1353.2	1418.2	n.m.	n.m.	1.008	0.005	n.m.	n.m.	-16.3	0.5
ATQ 205	51.50	17.80	n.m.	n.m.	0.979	0.003	n.m.	n.m.	n.m.	n.m.	792.2	725.9	n.m.	n.m.	1.003	0.002	n.m.	n.m.	-9.3	0.5
ATQ 206	8.29	11.54	n.m.	n.m.	0.967	0.003	n.m.	n.m.	n.m.	n.m.	296.8	335.7	n.m.	n.m.	0.993	0.001	n.m.	n.m.	n.m.	0.5
ATQ 207	0.33	11.54	n.m.	n.m.	1.042	0.003	n.m.	n.m.	n.m.	n.m.	233.5	20.3	n.m.	n.m.	1.034	0.001	n.m.	n.m.	-14.2	0.5
RDC 300	104.99	47.19	n.m.	n.m.	0.904	0.018	n.m.	n.m.	-58.9	0.1	490.9	85.0	n.m.	n.m.	0.926	0.004	n.m.	n.m.	-7.3	0.6
RDC 306	60.59	12.61	n.m.	n.m.	1.027	0.007	n.m.	n.m.	n.m.	n.m.	917.0	161.9	n.m.	n.m.	1.023	0.001	n.m.	n.m.	-8.9	0.5
RDC 308	0.33	0.09	0.43	0.01	n.m.	n.m.	0.666	0.005	n.m.	n.m.	348.6	99.3	41.7	0.8	0.884	0.004	0.907	0.009	-13.2	0.5
RDC 309	1.12	1.12	n.m.	n.m.	n.m.	n.m.	n.m.	n.m.	n.m.	n.m.	490.5	170.5	n.m.	n.m.	0.866	0.004	n.m.	n.m.	-14.6	1.2
RDC 310	97.92	23.92	0.32	0.02	0.804	0.005	0.803	0.007	-65.9	0.1	600.3	48.2	89.2	1.8	0.886	0.006	0.954	0.009	-12.5	0.5
RDC 311	0.33	0.00	n.m.	n.m.	n.m.	n.m.	n.m.	n.m.	n.m.	n.m.	375.3	3.8	n.m.	n.m.	0.918	0.001	n.m.	n.m.	-9.5	0.5
RDC 312	198.87	163.70	n.m.	n.m.	0.845	0.035	n.m.	n.m.	-56.0	1.8	1012.4	292.1	n.m.	n.m.	0.864	0.006	n.m.	n.m.	-5.9	5.0
TOO 005	89.33	0.89	n.m.	n.m.	1.023	0.002	n.m.	n.m.	n.m.	n.m.	815.9	8.2	n.m.	n.m.	1.014	0.002	n.m.	n.m.	n.m.	n.m.
TOO 006	0.26	0.01	n.m.	n.m.	n.m.	n.m.	n.m.	n.m.	n.m.	n.m.	466.2	4.7	n.m.	n.m.	0.855	0.002	n.m.	n.m.	n.m.	n.m.
INI 001	0.07	0.01	n.m.	n.m.	n.m.	n.m.	n.m.	n.m.	n.m.	n.m.	85.1	0.9	n.m.	n.m.	1.038	0.003	n.m.	n.m.	n.m.	n.m.

INI 004	0.13	0.01	n.m.	n.m.	n.m.	n.m.	n.m.	n.m.	n.m.	n.m.	3.2	0.0	n.m.	n.m.	0.888	0.091	n.m.	n.m.	n.m.	n.m.
INI 005	0.40	0.01	n.m.	n.m.	n.m.	n.m.	n.m.	n.m.	n.m.	n.m.	323.7	3.2	n.m.	n.m.	1.033	0.004	n.m.	n.m.	n.m.	n.m.
L9811	0.79	0.01	n.m.	n.m.	0.814	0.042	n.m.	n.m.	n.m.	n.m.	1118.5	11.2	n.m.	n.m.	0.951	0.003	n.m.	n.m.	n.m.	n.m.
INI 003	54.31	0.54	n.m.	n.m.	1.006	0.004	n.m.	n.m.	n.m.	n.m.	894.8	8.9	n.m.	n.m.	1.002	0.004	n.m.	n.m.	n.m.	n.m.
INI 006	0.46	0.01	n.m.	n.m.	0.847	0.102	n.m.	n.m.	n.m.	n.m.	94.2	0.9	n.m.	n.m.	n.m.	n.m.	n.m.	n.m.	n.m.	n.m.
IKP 003	91.71	0.92	n.m.	n.m.	1.020	0.006	n.m.	n.m.	n.m.	n.m.	298.4	3.0	n.m.	n.m.	1.032	0.008	n.m.	n.m.	n.m.	n.m.
IKP 001	0.13	0.01	n.m.	n.m.	n.m.	n.m.	n.m.	n.m.	n.m.	n.m.	127.6	1.3	n.m.	n.m.	0.965	0.006	n.m.	n.m.	n.m.	n.m.
TES 001	0.26	0.01	n.m.	n.m.	n.m.	n.m.	n.m.	n.m.	n.m.	n.m.	439.6	4.4	n.m.	n.m.	0.928	0.006	n.m.	n.m.	n.m.	n.m.
TES 004	0.40	0.01	n.m.	n.m.	n.m.	n.m.	n.m.	n.m.	n.m.	n.m.	67.9	0.7	n.m.	n.m.	1.002	0.004	n.m.	n.m.	n.m.	n.m.
TES 006	1.06	0.01	n.m.	n.m.	0.791	0.030	n.m.	n.m.	n.m.	n.m.	840.6	8.4	n.m.	n.m.	0.934	0.003	n.m.	n.m.	n.m.	n.m.
UMI 001	n.m.	n.m.	n.m.	n.m.	n.m.	n.m.	n.m.	n.m.	n.m.	n.m.	510.7	5.1	n.m.	n.m.	0.971	0.003	n.m.	n.m.	-10.7	0.5
UMI 003	68.18	0.68	n.m.	n.m.	0.988	0.003	n.m.	n.m.	-67.4	0.1	500.0	5.0	n.m.	n.m.	1.005	0.003	n.m.	n.m.	-8.4	0.5
UMI 005	56.82	0.57	n.m.	n.m.	1.027	0.003	n.m.	n.m.	-73.3	0.1	216.9	2.2	n.m.	n.m.	1.048	0.003	n.m.	n.m.	-12.3	0.5
UMI 006	4.36	0.04	n.m.	n.m.	n.m.	n.m.	n.m.	n.m.	n.m.	n.m.	295.1	3.0	n.m.	n.m.	1.007	0.004	n.m.	n.m.	n.m.	n.m.

Table S3: Organic carbon content of North Slope sediments.

Percent organic carbon (OC) data collected from a sediment exposure at the boundary of the eolian silt and eolian sand geologic units on the North Slope of Alaska (69°51'5.84"N, 154°51'48.26"W). Because of its location, this approximately 45-m-thick sedimentary exposure has two main sedimentary units representative of the eolian sand and eolian silt geologic zones that underlie several of the study lakes. The average OC content is 0.19 ± 0.10 % for the sand and 0.95 ± 0.34% for the silt (mean ± std., n = 29 - 38).

Eolian Sand Sample ID	**OC** % mass	**Eolian Silt** Sample ID	**OC** % mass
CAR-1-10	0.188	CAR-1-0	0.387
CAR-1-20	0.192	CAR-2-0	0.485
CAR-1-30	0.186	CAR-2-5	0.529
CAR-1-40	0.171	CAR-2-20	0.393
CAR-1-50	0.175	CAR-2-25	0.491
NC 0	0.143	CAR-2-30	0.475
NC 0.5	0.156	CAR-2-40	0.421
NC 1	0.182	NC 7.31	0.452
NC 1	0.14	NC 9.5	1.886
NC 1	0.185	NC 10	0.949
NC 2	0.123	NC 10.5	0.922
NC 2.5	0.12	NC 11	1.228
NC 3	0.234	NC 11	1.249
NC 4	0.118	NC 11	1.067
NC 4.5	0.171	NC 11.5	1.154
NC 5	0.115	NC 12	1.601
NC 5	0.112	NC 12.5	0.83
NC 5	0.138	NC 13	1.199
NC 23.5	0.353	NC 13.5	1.153
NC 24	0.27	NC 14	1.131
NC 24.5	0.102	NC 14.5	1.043
NC 25	0.283	NC 15	1.297
OC 2.5	0.164	NC 15.5	0.875
OC 3	0.318	NC 16	0.873
OC 3.5	0.151	NC 16.5	0.918
OC 4	0.354	NC 17	1.036
OC 4.5	0.177	NC 17.5	0.964
OC 4.5	0.163	NC 18	0.899
OC 4.5	0.174	NC 18	0.83
		NC 18	0.907
		NC 18.5	0.899
		NC 19	1.001
		NC 19.5	0.903
		NC 20	0.846
		NC 20.5	0.968
		NC 21	0.861
		NC 21.5	1.584
		NC 22	1.283

Table S4: Summary of Statistical Tests and Values.

All statistical tests were performed with the Microsoft data analysis package in Microsoft Excel 2010. All statistical tests are considered significant at the 0.05 level. n.a. = not applicable.

Test Variables	Statistical Test	F values	P values	T Critical, T Stat	Degrees of Freedom	R^2
^{14}C age differences (CH_4 and CO_2) across geologic units	Single-factor ANOVA and Tukey-Kramer HSD	CH_4: (4,21) = 19.49	7.92×10^{-7}	n.a.	25	n.a.
		CO_2: (4,30) = 10.85	1.46×10^{-5}	n.a.	34	n.a.
% Organic C in Sand vs. Silt sediments	Two-Tailed T-Test	n.a.	9.81×10^{-18}	2.0, -11.8	65	n.a.
Winter 2013 vs. Winter 2014 (dissolved CH_4 and CO_2 ages)	Paired Two-Tailed T-Test	n.a.	CH_4: 0.012	2.2, 3.0	11	n.a.
		n.a.	CO_2: 0.616	2.1, 0.51	18	n.a.
Winter 2014 vs. Summer 2014 (dissolved CH_4 and CO_2 ages)	Paired Two-Tailed T-Test	n.a.	CH_4: 0.049	2.57, 2.59	5	n.a.
		n.a.	CO_2: 0.009	2.6, 4.1	5	n.a.
Average age of CH_4 vs. CO_2 in Winter	Regression Analysis	167.26	2.61×10^{-12}	n.a.,12.93	25	0.87
[CH_4] vs. $\delta^{13}CH_4$ in winter 2013 & 2014 (if $\delta^{13}CH_4 > -60$ ‰)	Regression Analysis	2013: 2.91	0.23	n.a., -1.70	3	0.59
		2014: 51.12	8.32×10^{-4}	n.a., -7.15	6	0.91

Supplementary Information References:

61. Grosse, G., Jones, B. M. & Arp, C. D. in *Treatise on Geomorphology* (eds. Shroder, J. F., Giardino, R. & Harbor, J.) 325–353 (Elsevier Inc., 2013).